ASTROPHYSICAL JETS

BY DAVID A. CLARKE, NICHOLAS R. MACDONALD, JON P. RAMSEY AND MARK RICHARDSON

Astrophysical jets are long, collimated, supersonic flows of plasma emanating from compact celestial objects such as *protostellar objects* (PSO) that become stars once thermonuclear reactions begin, and *active galactic nuclei* (AGN) that are supermassive black holes ($10^8 - 10^9\ M_\odot$, where $M_\odot = 2 \times 10^{30}$ kg is the mass of the sun) at the cores of nascent galaxies. Examples of jets are shown in Fig. 1. "Dead stars" (white dwarfs, neutron stars, and stellar black holes) can also exhibit jets (*e.g.*, the famous microquasar SS433 [1]), but we shall concentrate here on jets from "young" objects such as PSO and AGN.

The term *jet* was first applied to an astronomical object by Baade & Minkowski [2] to the "protrusion" out of the core of the nearby galaxy M87. In fact, this feature was first observed by H. Curtis in 1918 [3], the same Curtis of the famous "Curtis-Shapley debate" [4]. By the late 1980s, dozens of extragalactic radio jets had been extensively studied (*e.g.*, http://www.jb.man.ac.uk/atlas), most with radio interferometers such as the National Radio Astronomy Observatory's Very Large Array, although several have been observed optically with the Hubble Space Telescope (HST) [5] and a few in x-rays (*e.g.*, Wilson *et al.* [6]).

SUMMARY

Nature has devised numerous mechanisms by which the universe could become self-aware, and where humanity could spring forth from the ashes of ancient supernovæ and gaze back upon the heavens to contemplate its origins. Astrophysical jets are one such mechanism. To an astronomer, a jet is a long, collimated, supersonic flow of gas emanating from a condensed object collapsing under its own weight. But to a forming star, a jet is the "arm" by which angular momentum is removed from the rapidly rotating object, allowing it to evolve. Without this mechanism, the spin of a protostar would prevent it from collapsing enough to trigger thermonuclear fusion, and we would not be here to talk about it.

In this contribution, we introduce the reader to astrophysical jets, and discuss how supercomputing allows us to investigate the physics of these "hand-brakes of nature".

What are now known as PSO jets can be traced to S. Burnham's discovery in 1890 [7] of what he called "faint nebulosities". Burnham's objects were first interpreted as faint stars, but later identified as a separate class of objects by G. Herbig and G. Haro in the 1940s and for whom these objects are now named. Herbig-Haro (HH) objects were not widely understood as jets until the early 1980s when observations first revealed their narrow and collimated nature (*e.g.*, Snell *et al.* [8] use the term "streams", and don't go quite so far as to call them "jets"). Hundreds of HH objects are now known, many of them associated with jets (http://casa.colorado.edu/hhcat).

As protostars and protogalaxies form, the surrounding gas, dust and, in the case of the latter, whole stars are drawn in gravitationally which, by necessity, possess *some* initial angular momentum. As collapse ensues, conservation of angular momentum requires that the rotation speed of the in-falling material increases until it reaches a point—the so-called *centrifugal barrier*—where it can no longer move toward the rotation axis. Instead, material may only

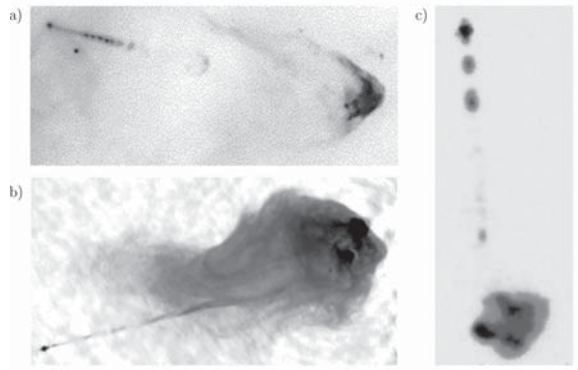

Fig. 1 Three "inverted palette" images of jets, where black represents the highest brightness. a) *Very Large Telescope* image of HH 34 in Orion (courtesy, the European Southern Observatory). The jet is the narrow feature emanating from the protostar in the top left corner and disappears from view before reaching its terminus at the right where it excites a *bow shock* in the interstellar medium; b) *Very Large Array* (VLA) image of the western jet in Cygnus A (from [9]). The jet moves from the AGN at the bottom left corner to the right filling a giant *radio lobe* of hot plasma (see [10] for an excellent overview of this prototypical AGN); c) VLA image of the "naked" jet from the quasar 1007+417. The quasar is the dark spot at the top of the image, and the jet is the series of knots ending at the small, off-axis lobe at the bottom.

D.A. Clarke <dclarke@ap.smu.ca>, N.R. MacDonald, J.P. Ramsey, and M. Richardson, Institute for Computational Astrophysics, Department of Astronomy & Physics, Saint Mary's University, Halifax, Nova Scotia, Canada, B3H 3C3

"fall" parallel to the axis and on to the equatorial plane, forming an *accretion disc*. Were there no way for the disc to lose any of its angular momentum, such a configuration would remain stable for æons, rotating in a pseudo-solid body/Keplerian fashion much like the Milky Way does, without forming a compact object—the star or AGN—at its centre. Planets would not form from the debris of the disc, and we would not be here to discuss it.

But Nature has found a way to rid the system of its angular momentum—jets. As shown in Fig. 2, a small fraction of the disc material is thrown off in long, collimated, oppositely-directed supersonic outflows carrying with them most of the disc's angular momentum. This allows material in the disc to drift inward and collect at the gravitational "bottom" of the system (*e.g.*, Königl & Pudritz [11]; Shu *et al.* [12]). Remarkably this process has been directly observed. Table 1 gives recent results from Woitas *et al.* [13] for the PSO RW Auriga. In these HST observations, the jet and accretion disc are sufficiently resolved to measure rotational speeds from Doppler-shifted emission lines. From these data and previous measurments of mass flow rates, angular momentum fluxes are deduced. The conclusion: the jets in RW Aur transport less than ten percent of the accreted material but more than 2/3 of the angular momentum away from the disc.

TABLE 1

Measured rates at which mass and angular momentum are accumulated on the accretion disc (inflow) and then transported away by jets (outflow) for RW Aur (from [13]). An AU (Astronomical Unit) is 1.5×10^8 km, the distance between the Earth and the sun.

	$\dot{M}$	$\dot{L}$
inflow	$(1.77 \pm 0.12) \times 10^{-6}\ M_\odot\ \mathrm{yr}^{-1}$	$(6.6 \pm 1.5) \times 10^{-5}\ \mathrm{AU}\, M_\odot\ \mathrm{km\,s}^{-1}\ \mathrm{yr}^{-1}$
outflow	$(0.17 \pm 0.02) \times 10^{-6}\ M_\odot\ \mathrm{yr}^{-1}$	$(4.8 \pm 1.8) \times 10^{-5}\ \mathrm{AU}\, M_\odot\ \mathrm{km\,s}^{-1}\ \mathrm{yr}^{-1}$

Even before remarkable observations such as Woitas *et al.* were possible, jets were known to be associated with most star formation regions as well as young galaxies and quasars, and it has been widely believed for some time that virtually all stars and AGNs pass through a "jet phase" (*e.g.*, see [14] for a recent and very digestible review of jets). A typical AGN is 10^8 times more massive than a PSO, and thus the scales of their associated jets are much greater. Jets from PSOs are about a light year (10^{16} m) in length and travel at 100–200 km/s, while those from AGNs can be longer than 10^6 light years and travel at 90% or more the speed of light. The jet phase might last 10^5 yr for a PSO and 10^8 yr for an AGN; in either case, a very small fraction of their total lifetime.

Besides their size, one of the most important differences between jets from PSOs and AGNs is their density relative to their surrounding media. The density of a typical galactic jet is ~10^4 particles per cm^3 (an excellent laboratory vacuum is 10^4 times denser), similar to that of the surrounding interstellar medium (ISM) for a density ratio of ~1. Conversely, a typical extragalactic jet may have a density of only 1 m^{-3} (that's per cubic *metre*) while that of the surrounding inter-galactic medium (IGM) ~1 cm^{-3} for a density ratio of 10^{-6}. It is this striking difference in density ratios that is thought to be responsible for many of the morphological differences between galactic and extragalactic jets.

Prior to 1985, a prevailing model for launching outflows posited that a *thick accretion disc*—one whose "vertical" thickness is an appreciable fraction of its equatorial radius—formed about a compact object with a deep "funnel" reaching down to the object's surface. A radiation-driven wind from the compact object would be blocked by the disc in the equatorial plane, but allowed to escape along the rotation axis and within the evacuated funnel. Indeed, the funnel would help collimate the outflow into the narrow jets observed [15,16]. However, in 1985 Papaloizou & Pringle [17] showed that such a funnel is hydrodynamically unstable in 3-D, rendering the mechanism impotent.

It was Blandford & Payne [18] who first described the jet-launching model to stand the test of time. They showed that a jet can be launched *magneto-centrifugally* from the surface of an accretion disc, much like a bead on a wire accelerates outward if the wire were slanted outward enough from the rotation axis, then spun about. In this model, the "bead" is a mass of hot, ionised plasma and the "wire" is a magnetic field line. As ionised matter cannot cross field lines, it is obliged to follow it and thus form a collimated jet (Fig. 2).

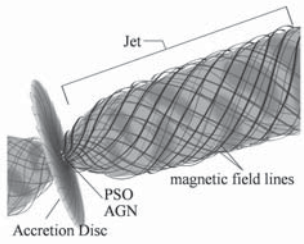

Fig. 2. Artist's rendition of the Blandford & Payne model, in which the rotating accretion disc wraps up magnetic field lines into a helical pattern, launching a jet from the surface of the disc [courtesy NASA/ESA and Ann Feild (STScI)].

This paper inspired other theoretical discussions (*e.g.* [19,20]), and numerous computational investigations (*e.g.*, [21–27]) to study various aspects of this theory. While each of these works examined the problem from a different angle, all agree on one main point: *In a rotating, magnetised plasma collapsing under its own gravity, jets are unavoidable.*

THEORY AND METHODOLOGY

Jet Physics

It is often said that 98% of the universe is in the plasma state, with the Earth—in its mostly solid state—representing an anomaly. Plasma physics is enormously complicated to solve properly as it requires tracking every particle—ion—under their mutual electromagnetic and, in astrophysics, gravitational

fields. Fortunately, if one can assume charge neutrality over small volumes of space and that relative speeds among the particles are comfortably sub-light, a simpler system of equations—those of *magnetohydrodynamics* (MHD)—prevail.

MHD was almost single-handedly developed by the Swedish physicist Hannes Alfvén (1908–1995) who won the Nobel prize for his efforts in 1970 (http://public.lanl.gov/alp/plasma/people/alfven.html). His was often the story of "the lone voice in the wilderness", where scoffs such as 'Were such a thing possible, Maxwell himself would have discovered it!' were reportedly heard at his seminars. It wasn't until Enrico Fermi, having attended one of Alfvén's lectures, pronounced his theory to be sound that Alfvén's ideas started to be taken seriously. And when his most controversial prediction—that a form of electromagnetic waves, later to be known as *Alfvén waves*, could propagate through a conducting medium—was confirmed in the lab in the late 1950s, his ideas finally became mainstream.

In their *primitive form*, the equations of ideal (infinite conductivity) MHD are:

$$\frac{\partial \rho}{\partial t} + \nabla \cdot (\rho \vec{v}) = 0; \tag{1}$$

$$\frac{\partial \vec{v}}{\partial t} + (\vec{v} \cdot \nabla)\vec{v} = -\frac{1}{\rho}\nabla p - \nabla\phi + \frac{1}{{}_0\rho}(\nabla \times \vec{B}) \times \vec{B}; \tag{2}$$

$$\frac{\partial p}{\partial t} + \vec{v} \cdot \nabla p = -\gamma p \nabla \cdot \vec{v} \tag{3}$$

$$\frac{\partial \vec{B}}{\partial t} = \nabla \times (\vec{v} \times \vec{B}), \tag{4}$$

where ρ is the density, $\vec{v}$ is the fluid velocity, $p \propto \rho^{\gamma}$ is the thermal pressure, γ is the ratio of specific heats (5/3 for a plasma), ϕ is the gravitational potential satisfying Poisson's equation ($\nabla^2\phi = 4\pi G\rho$), and $\vec{B}$ is the magnetic induction which, by virtue of equation (4), satisfies the solenoidal condition, $\nabla \cdot \vec{B} = 0$, for all time so long as it is imposed as an initial condition.

These equations reduce to those of ordinary fluid dynamics when $\vec{B} = 0$. They describe how fluid—ionised gas in this case—flows under the influence of pressure gradients, gravity, and magnetic forces. It is an extremely rich and non-linear system of equations permitting four types of waves, both longitudinal and transverse. Except for the simplest of situations, they are almost completely inscrutable by pen and paper, and computational methods are necessary to make progress in realistic systems. Introductions to the subject can be found in the texts by Davidson [28] and Biskamp [29].

Jets are a classic astrophysical application of MHD. The MHD approximation (isotropic pressure, local charge neutrality, sub-light interparticle speeds) is widely believed to be valid, and there is much evidence of the association of jets with diffuse gases and magnetic fields [14]. We therefore use equations (1)–(4) as our starting point to build our jet models.

Computational Methods

We use *ZEUS*-3*D*, a computer program under development by the authors at the ICA and publicly available on the ICA web site (http://www.ica.smu.ca/zeus3d). A comprehensive user manual and a gallery of 1-D, 2-D and 3-D simulations are also available from this site, and inquiries on its use should be directed to DAC.

ZEUS-3*D* is an example of a *finite-volume* code in which a region of interest—say the portion of the ISM or IGM through which a jet propagates—is divided into a number of small *zones*, typically 100 million or more in 3-D. Equations (1)–(4), or at least their *conservative* variations (*e.g.* [30]), are integrated over each zone volume and/or zone face and the resulting *difference* equations are advanced in time by a small *time-step* using a time-centred and conservative procedure. This process is repeated for as many time-steps as required (*e.g.*, tens of thousands) until the system has evolved to the desired state. As for any system of partial differential equations, initial and boundary conditions define the problem and for us, these are set to launch a jet from the surface of an accretion disc, or propagate a jet through a quiescent medium. The truly dedicated reader can find a complete description of the numerical methods in Clarke [31].

THE SIMULATIONS

Magneto-centrifugally Launched Jets

Figure 3 illustrates our initial conditions for launching a jet from the surface of an accretion disc (inner radius $r_i \sim 0.05$ AU). An atmosphere in hydrostatic equilibrium ($\rho_{atm} \sim r^{-1/(\gamma-1)}$) is established about a 1 $M_{\odot}$ central mass (PSO) that provides the gravity. A hydrostatic disc in Keplerian rotation about the PSO is maintained as left boundary conditions, with $\rho_{disc}/\rho_{atm} = 100$ and $p_{disc}/p_{atm} = 1$ (pressure balance). A uniform magnetic field [$B_z^2 = 0.05\mu_0 p(r_i)$] perpendicular to the disc permeates both the atmosphere and the disc. At $t = 0$, the disc is suddenly set into rotation and a rather knotty jet is the result (Fig. 4). The initial B_z is wrapped around the rotation axis creating the helical field needed for the Blandford & Payne mechanism to accelerate material along the z (horizon-

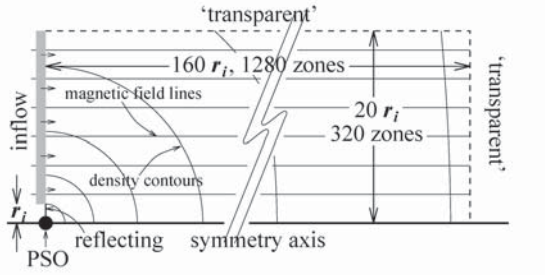

Fig. 3 Schematic diagram showing the initialisation of the magneto-centrifugally launched jet problem with all boundary types labeled. The disc is the gray band along the left side, with the inner radius of the disc, r_i, shown.

Fig. 4. A 2-D axisymmetric simulation of a jet flowing from left to right and launched from an accretion disc maintained as boundary conditions on the left side. The top half shows density and the bottom half B_ϕ, with black indicating high values, white low values. Note that the density "knots" correspond to regions of relatively low B_ϕ.

tal) axis.

As tempting as the association may be between the knotty appearance of the jet in HH 34 (Fig. 1*a*) and the knots (actually "rings" in axisymmetry) in the simulated jet (Fig. 4), it is unlikely these two phenomena are related, at least directly. Figure 4 represents the first 8 AU (~ 1 light-*hour*) of the jet, whereas the HH 34 jet is about 1 light-*year* in length. Instead, (magneto)hydrodynamical instabilities within the jet itself (*e.g.*, shocks) are likely the cause of the HH 34 knots, although they could well begin as the knots seen in Fig. 4. Indeed, this points to a current limitation of all simulations performed to date: *No single simulation has yet been able to resolve the jet launching region and follow the jet to observable scale lengths*. This is a very difficult computational problem, and one that is at the core of the Ph.D. dissertation of JPR.

Still, the origin of the knots in the simulation is of interest (*e.g.* [32]), as they point to an important role played by the protostellar atmosphere not considered in the original Blandford & Payne model. Figure 5 shows the density distribution, magnetic field lines, velocity vectors, and acceleration vectors of the inner-most region of our simulation (0.4 × 0.5 AU) at a time that best illustrates how the knots are formed.

Because the disc has an *inner* radius, r_i, the Blandford & Payne mechanism is capable of launching material from the disc at $r > r_i$ only. As material begins moving away from the disc, the hydrostatic balance of the atmosphere is disturbed and, at least at first, gravity wins out. Material, particularly near the axis, is drawn toward the centre (*e.g.*, some of the white velocity vectors along the axis in Fig. 5 are pointing inward), replenishing the central core with material. The momentum of the inwardly falling material actually adds more matter to the core than needed to restore balance, and the imbalance in hydrostatic equilibrium now favours the outward pressure gradient. This drives material away from the core but, owing to the still inwardly moving material close to the axis, is redirected to lower latitudes (upward in Fig. 5), forming the rings, or knots. This time, momentum carries too much material away from the core so that gravity is again dominant, and the process repeats like a damped, driven oscillator continuing for as long as the simulation is run. From the local accelerations (black vectors in Fig. 5) and densities, we can deduce the period of oscillation

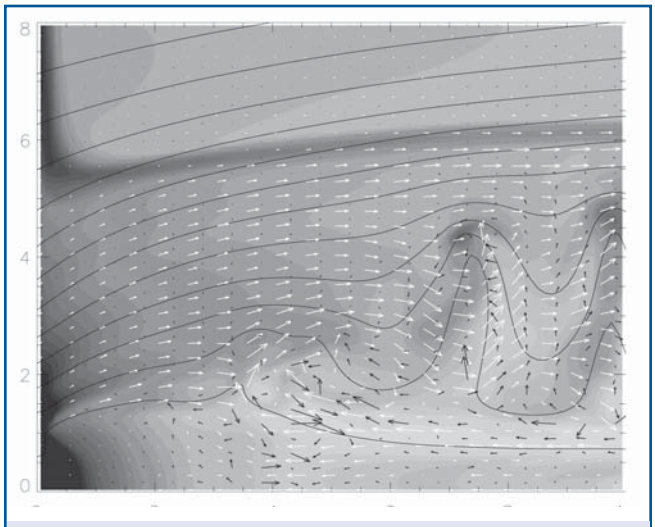

Fig. 5. A blow-up of the inner $8r_i$ x $10r_i$ (0.4 × 0.5 AU) of the launched jet, showing details of how the knots are generated. Greyscale is density with black indicating high values, black lines are magnetic field lines, white arrows indicate velocities, while black arrows show accelerations. The disc is located along $x_1 = 0$ and $x_2 \geq 1$, where x_1 and x_2 are the axial (z) and radial (r) coordinates respectively. The putative protostar is located at the origin.

and, with the local velocities, we can determine the expected spacings between the knots. We find this agrees with the measured spacings in the simulations to within 10–20%.

Of course, the role of the magnetic field is critical for all aspects of this calculation, including the condensation of the knots. Much of the knot material originates from near the axis where B_ϕ is the lowest (the ϕ-component of any vector must go to zero toward a symmetry axis). As this material is pushed to lower latitudes, the paucity of B_ϕ within the knot means its combined magnetic and thermal pressure is lower than that of its new surroundings, and it is compressed into the high density, low B_ϕ features we see in Fig. 4.

The knots represent a significant modification to the Blandford & Payne model, one that only numerical simulations could reveal. While these knots may not be directly related to the observed knots (though we won't know this for sure until we do the calculations), they do have quantitative implications on the mass and momentum fluxes transported by the jet which, in these simulations, are still too low by a factor of two to ten compared with measured fluxes from a typical stellar jet. Reasons for this discrepancy may include:

1. the disc we impose as left boundary conditions may be unrealistic;
2. starting the simulation off with the disc suddenly rotating at $t = 0$ rather than allowing the disc and jet to co-evolve may have unrealistic consequences;
3. our initial atmosphere, which we know plays a critical role in the oscillatory nature of the knot generator, is

probably unrealistic;

4. our disc extends only to 1 AU and yet in our own solar system, the solar disc extended at least to Neptune (30 AU), and probably much further.

It is for these reasons that we are taking the next step, and doing a simulation to include the jet launching region, the entire disc, and more realistic initial atmospheric and magnetic configurations on a grid that will extend to observed scale lengths (10^4–10^5 AU). This should give us a great deal more insight into the nature of stellar jets and what, if anything, their observed properties can tell us about the conditions where they were launched.

Propagating Jets

We are also studying the effects of magnetism on an extragalactic jet propagating through the IGM. As shown in Fig. 6, we initialise a uniform, quiescent unmagnetised ambient medium and inject a light ($\rho_{jet}/\rho_{amb} \equiv \eta = 0.02$), supersonic ($M = 10$ is the *Mach number*, the ratio of the jet speed and local sound speed) and magnetised jet, as indicated by the arrow at the bottom left corner of the figure. We do not concern ourselves here with *how* the jet is launched, just how the jet, once launched, interacts with its surroundings.

Questions to address include: What is the nature of the

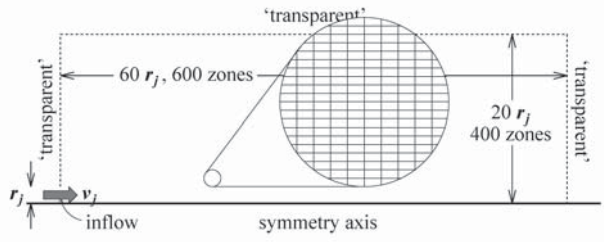

Fig. 6 Schematic diagram showing the initialisation of the propagating jet problem (r_j = jet radius, v_j = jet velocity) with all boundary types labeled. The inset indicates the scale of the elongated zones used for both the launched jet and propagating jet problems, where the elongation is in the direction of flow.

"hotspots" in AGN lobes such as Cygnus A (Fig. 1*b*)? How does the magnetic field affect the appearance of the jet-lobe system? What is the origin of the filaments observed in Cygnus A and many other AGN lobes? Some of these questions are fairly well understood, some are still open. In either case, this is an area where numerical simulations have taken the lead role.

The early 2-D axisymmetric simulations of Norman *et al.* [33] contributed two very important pieces of insight. First, the hot spots at the lobe extremities mark a strong shock where the supersonic jet flow is decelerated to subsonic speeds. Kinetic energy is converted to magnetic and thermal energy, and these increase the synchrotron emissivity (the primary emission

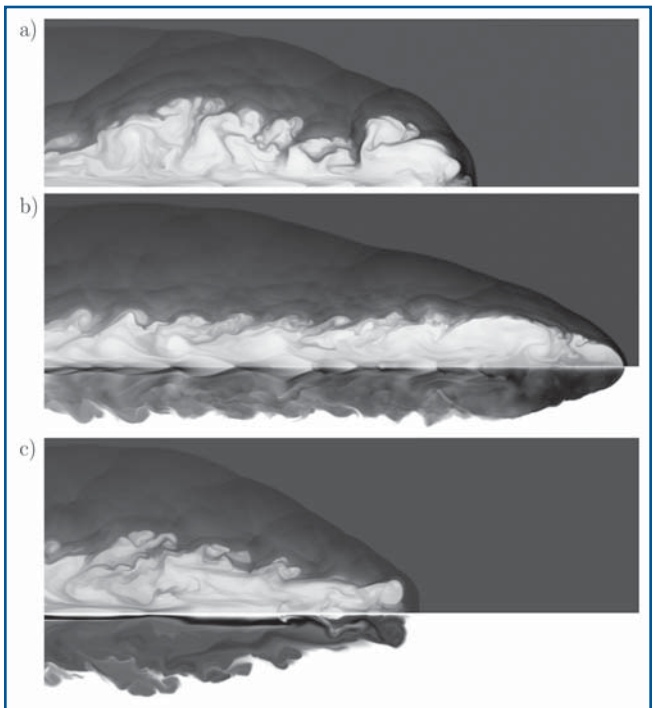

Fig. 7. a) Density distribution for a 2-D axisymmetric jet with a very weak magnetic field; b) Density (upper) and B_ϕ (lower) for a 2-D jet with a strong B_ϕ; c) Density (upper) and A_ϕ (lower) for a 2-D jet with a strong B_p. In all cases, black indicates high values, white zero.

mechanism for extragalactic jets) dramatically in the hot spots and lobes. Second, they found that dense jets ($\eta > 1$) are "naked" while light jets ($\eta < 1$) enshroud themselves in a *cocoon* or *lobe*. This computational observation along with the astronomical observation that most AGN jets feed extended "fluffy" lobes is the primary reason why it is believed that $\eta \ll 1$ for most extragalactic jets.

Figure 7 shows three M = 10, $\eta = 0.02$ jets at the same evolutionary time that differ only in the nature of the magnetic field they transport. Panel (*a*) depicts a jet with a weak magnetic field, (*b*) a jet with a strong *toroidal* magnetic field ($\beta_{tor} \equiv 2\mu_0 p/B_\phi^2 = 0.2$), and (*c*) a jet with a strong *poloidal* magnetic field ($\beta_{pol} \equiv 2\mu_0 p/B_p^2 = 0.2$, where $B_p^2 = B_r^2 + B_z^2$). Panel (*b*) includes both density (upper) and B_ϕ (lower), whereas panel (*c*) includes both density (upper) and the ϕ-component of the vector potential, A_ϕ (lower), whose contours follow magnetic field lines.

All flow is from left to right, with the actual *jet* confined to near the symmetry axis. In Fig. 7*a*, for example, the jet streams along the bottom 1/20 of the image and is characterised by several condensations (grey knots) along the axis from which oblique shocks (grey streaks pointing to the left) are anchored. The large light-grey and turbulent region above the jet is the cocoon filled with exceedingly hot (~10^9 K) jet material that passed through the *Mach disc* at the jet terminus. The bow

shock leading the jet and surrounding the cocoon is in the ambient medium, and the sharp separation between the light grey cocoon and the dark grey shocked ambient medium is the *contact discontinuity*. This is known to be *Kelvin-Helmholtz unstable*, whence the many undulations and "fingers" of ambient medium reaching into the cocoon.

Consider first the jet with the weak magnetic field in Fig. 7*a*. If this jet were ballistic, it would have propagated eleven times the distance shown. Instead, with $\eta = 0.02$, this jet resembles a jet of compressed air in water; it manages to advance, but results in a lot of backflow, internal shocks, and an extended and turbulent cocoon [33].

On the other hand, the *hoop-stress* of a strong toroidal magnetic field provides rigidity even to a light jet, allowing the jet to present a "sharper" leading point as it propagates [34]. Thus, the jet in Fig. 7*b* advances further with less back-flowing material and a narrower cocoon. The opposite is true with the poloidal field jet. Large poloidal *flux loops* form at the head of the jet and "peel away" from the axis giving the jet a "blunter" presentation than even the hydrodynamical jet. Progress is correspondingly slower and more material is deflected into the cocoon. In Fig. 7*c*, the cocoon is as narrow as it is because of the "transparent" boundary conditions above the jet inlet (Fig. 6) and most of the cocoon material flows off the grid at the left side. Were reflecting conditions imposed, this material would remain on the grid and the cocoon would be substantially larger.

Finally, Fig. 8 shows line-of-sight integrations of the synchrotron emissivity of two 3-*D* simulations, and represent how a radio telescope might observe such objects. Figures 8*a* and 8*b* are, respectively, jets with a weak ($\beta_\phi = 10^5$) and strong ($\beta_\phi = 0.2$) toroidal magnetic field. Unlike 2-D, in 3-D the toroidal field is free to move off the initial symmetry axis, and the field is mostly poloidal in the cocoon. Both jets have $M = 10$ and $\eta = 0.1$, with η chosen higher than the 2-D jets to reduce computational time. Even still, each jet took several days on a 16-core, 2.4 GHz cluster to complete.

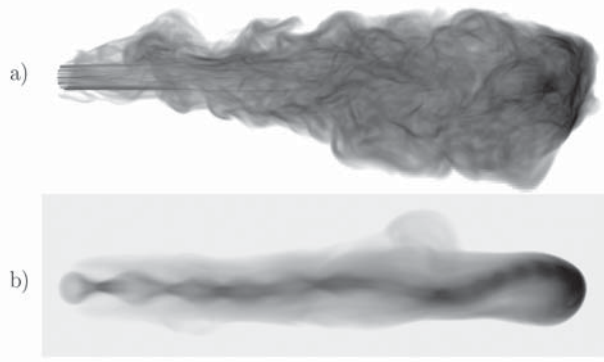

Fig. 8. Line-of-sight integrations of the synchrotron emissivity for two 3-D jet simulations with *a*) a dynamically weak magnetic field ($\beta \gg 1$), and *b*) with a dynamically strong toroidal magnetic field at the orifice. As with Fig. 1, these images are shown with inverted palettes.

The most striking aspect of Fig. 8*a* is the filamentary nature of the cocoon, and its similarity with the Cygnus A lobe in Fig. 1*b*. In the simulations, the filaments are a result of turbulent eddies in the lobe wrapping the weak magnetic field into bundles. This is such a fundamental property of weak-field turbulence, that one might expect *all* extragalactic radio lobes to be filamentary, and indeed all *well-resolved* (and thus near-by) radio lobes are (*e.g.*, Pictor A, M87, 3C 219, Centaurus A, to name the best-known).

However, some of the more distant radio lobes do not resemble Cygnus A. The lobe associated with the quasar 1007+417 (Fig. 1*c*) is not filamentary and is confined to the head of the jet. Superficially, it resembles Fig. 8*b*, suggesting 1007+417 may be an example of a jet transporting a strong toroidal magnetic field. Could qualities such as "extended and filamentary" *vs*. "confined and smooth" be indicators of local magnetic field strength?

Unfortunately, things are never so simple. Other 2-D and 3-D simulations show that a jet with a strong magnetic field can still have an extended, filamentary lobe provided it has a low enough η and high enough Mach number, M. On crossing the terminal jet shock (Mach disc), jumps in density and magnetic field asymptote to finite values as $M \to \infty$, while the jump in thermal pressure is unbounded. Thus, no matter how strong the field transported by the jet may be, a sufficiently strong shock can render the post-shock magnetic field dynamically weak, and the formation of an extended filamentary cocoon can result.

Further progress requires lots of computing power and an accurate MHD solver including as much physics as practical and possible. This includes a model for the emissivity that can exploit all the information the observations can yield. For example, synchrotron emission depends on the magnetic field and the relativistic electrons embedded in the fluid. The former we have, but we have had to make overly simplistic assumptions about the latter in creating Fig. 8. As part of his M.Sc. thesis, NRM is modifying ZEUS-3D to account for the energy gains and losses of the underlying electron population as it experiences the MHD effects of the overlying fluid. This will improve our ability to compare simulations with observations and untangle the competing physical effects responsible for the nature of extragalactic jets.

ACKNOWLEDGEMENTS

Support from NSERC though its DG, PGA, and USRA programmes is gratefully acknowledged. Some simulations were performed on facilities provided by the Atlantic Computational Excellence Network (ACEnet), funded by the CFI, ACOA, the provinces of Nova Scotia, Newfoundland & Labrador, and New Brunswick, and SUN Microsystems.

REFERENCES

1. K.M. Blundell and M.G. Bowler, *ApJ*, **616**, L159 (2004).
2. W. Baade and R. Minkowski, *ApJ*, **119**, 215 (1954).
3. H.D. Curtis, *Pub. Lick Obs.*, **13**, 31 (1918).
4. H. Shapley and H.D. Curtis, *Bull. of the Nat. Research Council*, **2**, 171 (1921).
5. W.B. Sparks, J.A. Biretta and F. Macchetto, *ApJS*, **90**, 909 (1994).
6. A.S. Wilson, A. Young and P.L. Shopbell, *ApJ*, **547**, 740 (2001).
7. S. Burnham, *MNRAS*, **51**, 94 (1890).
8. R.L. Snell, R.B. Loren and R.L. Plambeck, *ApJ*, **239**, L17 (1980).
9. R.A. Perley, J.W. Dreher, and J.J. Cowan, *ApJ*, **285**, L35 (1984).
10. C.L. Carilli and P.D. Barthel, *Astron. Astrophys. Rev.*, **7**, 1 (1996).
11. A. Königl and R.E. Pudritz, in *Protostars and Planets IV*, ed. V. Mannings *et al*., Tucson: Univ. Arizona Press, 759 (2000).
12. F.H. Shu, J.R. Najita, H. Shang and Z.-Y. Li, in *Protostars and Planets IV*, ed. V. Mannings *et al*., Tucson: Univ. Arizona Press, 789 (2000).
13. J. Woitas, F. Bacciotti, T.P. Ray, A. Marconi, D. Coffey and J. Eislöffel, *A&A*, **432**, 149 (2005).
14. E.M. de Gouveia Dal Pino, *Adv. in Space Research*, **25**, 908 (2005).
15. D. Lynden-Bell, *Phys. Scripta*, **17**, 185 (1978).
16. M.J. Rees, M.C. Begelman, R.D. Blandford, and E.S. Phinney, *Nature*, **295**, 17 (1982).
17. J.C.B. Papaloizou and J.E. Pringle, *MNRAS*, **213**, 799 (1985).
18. R.D. Blandford and D.G. Payne, *MNRAS*, **199**, 883 (1982).
19. R.E. Pudritz and C.A. Norman, *ApJ*, **301**, 571 (1986).
20. F.H. Shu, S. Lizano, S.P. Ruden and J. Najita, *ApJ*, **328**, L19 (1988).
21. G.V. Ustyugova, A.V. Kolboda, M.M. Romanova, V.M. Chechetkin and R.V.E. Lovelace, *ApJ*, **439**, 39 (1995).
22. R. Ouyed and R.E. Pudritz, *ApJ*, **484**, 794 (1997).
23. R. Krasnopolsky, Z.-Y. Li, and R.D. Blandford, *ApJ*, **526**, 631 (1999).
24. C. Fendt and D. Elstner, *A&A*, **363**, 208 (2000).
25. R. Ouyed, D.A. Clarke, and R.E. Pudritz, *ApJ*, **582**, 292 (2003).
26. J.M. Anderson, Z.-Y. Li, R. Krasnopolsky, and R.D. Blandford, *ApJ*, **630**, 945 (2005).
27. R. Banerjee and R.E. Pudritz, *ApJ*, **641**, 949 (2006).
28. P.A. Davidson, *An Introduction to Magnetohydrodynamics*, Cambridge University Press: Cambridge, ISBN 0 521 79487-0 (2001).
29. D. Biskamp, *Nonlinear Magnetohydrodynamics*, Cambridge University Press: Cambridge, ISBN 0 521 59918-0 (1997).
30. W. Dai and P.R. Woodward, *J. Comput. Phys*., **142**, 331 (1998).
31. D.A. Clarke, *ApJ*, **457**, 291 (1996).
32. R. Ouyed and R.E. Pudritz, *MNRAS*, **309**, 233 (1999).
33. M.L. Norman, L. Smarr, K.-H. Winkler, and M.D. Smith, *A&A*, **113**, 285 (1982).
34. D.A. Clarke, M.L. Norman, and J.O. Burns, *ApJ*, **311**, L63 (1986).